Letter

# Multidifferential study of identified charged hadron distributions in $Z$-tagged jets in proton-proton collisions at $\sqrt{s} = 13$ TeV

R. Aaij *et al.*[*]
(LHCb Collaboration)

(Received 5 September 2022; accepted 28 November 2022; published 4 August 2023)

Jet fragmentation functions are measured for the first time in proton-proton collisions for charged pions, kaons, and protons within jets recoiling against a $Z$ boson. The charged-hadron distributions are studied longitudinally and transversely to the jet direction for jets with transverse momentum $20 < p_{\mathrm{T}} < 100$ GeV and in the pseudorapidity range $2.5 < \eta < 4$. The data sample was collected with the LHCb experiment at a center-of-mass energy of 13 TeV, corresponding to an integrated luminosity of 1.64 fb$^{-1}$. Triple differential distributions as a function of the hadron longitudinal momentum fraction, hadron transverse momentum, and jet transverse momentum are also measured for the first time. This helps constrain transverse-momentum-dependent fragmentation functions. Differences in the shapes and magnitudes of the measured distributions for the different hadron species provide insights into the hadronization process for jets predominantly initiated by light quarks.

DOI: 10.1103/PhysRevD.108.L031103

Quarks and gluons can never be observed in isolation due to confinement in quantum chromodynamics (QCD). Thus, one of the challenges of QCD lies in relating the quark and gluon degrees of freedom of the theory to the bound-state hadrons observed in nature. A great deal of effort over the past several decades has gone into mapping out nucleon structure in terms of its quark and gluon constituents. A particular focus, in recent years, has been on the three-dimensional imaging of the nucleon [1,2]. Studying the mechanisms by which colored quarks and gluons hadronize into new color-neutral bound states offers complementary information connecting colored and hadronic degrees of freedom.

In the standard collinear perturbative QCD factorization framework, single-inclusive hadron production in proton-proton ($pp$) collisions factorizes into the short-distance hard scattering of partons and the long-distance dynamics described by fragmentation functions (FFs) and parton distribution functions (PDFs). The latter parametrizes proton structure as a function of momentum fraction carried by a parton of an incoming proton taking part in the hard scattering process. Hadronization of charged particles is described by collinear FFs, denoted as $D_q^h(z)$, where $z$ is the longitudinal momentum fraction of an outgoing parton $q$ carried by a produced hadron $h$ (see Ref. [3] for a review of FFs). The FFs and PDFs are not fully calculable perturbatively and must be constrained by experimental measurements. In Monte Carlo (MC) generators, phenomenological models tuned to data are used to perform hadronization. [4–6]. Jet fragmentation functions (JFFs) are experimental observables describing jet substructure that measure the longitudinal momentum fraction carried by a hadron of a jet [7–13]. Within the soft-collinear effective theory framework, JFFs are constructed such that they can probe the standard collinear FFs, defined for inclusive single-hadron production with no requirement of a reconstructed jet. Similarly, transverse-momentum-dependent (TMD) JFFs defined within the soft-collinear effective theory framework can access standard TMD FFs [14], traditionally measured in $e^+e^-$ collisions [15–20] and semi-inclusive deep inelastic lepton-nucleon scattering [21,22]. In addition to the dependence on the longitudinal momentum fraction $z$, TMD FFs also depend on $j_{\mathrm{T}}$, the transverse momentum of the produced hadron with respect to the jet axis in the case of a fully reconstructed jet, or the thrust axis in $e^+e^-$ collisions (see, e.g., Ref. [18]). Singly differential TMD JFFs for unidentified hadrons have previously been measured in proton-proton collisions at the LHC [23–26]. The excellent hadron identification capabilities at LHCb allow for measurements of the JFFs for different particle species.

This Letter presents the first measurements of JFFs for identified charged hadrons in jets produced in association with a $Z$ boson in the forward region of $pp$ collisions. The main observables are the longitudinal momentum fraction of the jet carried by the hadron, $z$, and the transverse

[*]Full author list given at the end of the article.



 

component of the hadron momentum with respect to the jet axis, $j_{\mathrm{T}}$, as found in Refs. [25,27] and defined as

$$z = \frac{\mathbf{p}_{\mathrm{had}} \cdot \mathbf{p}_{\mathrm{jet}}}{|\mathbf{p}_{\mathrm{jet}}|^2}, \qquad j_{\mathrm{T}} = \frac{|\mathbf{p}_{\mathrm{had}} \times \mathbf{p}_{\mathrm{jet}}|}{|\mathbf{p}_{\mathrm{jet}}|}, \tag{1}$$

where $\mathbf{p}_{\mathrm{had}}$ and $\mathbf{p}_{\mathrm{jet}}$ are the hadron and jet three-momentum vectors, respectively.

The dominant leading order hard process for $Z+\mathrm{jet}$ production in the LHCb acceptance is $qg \to Zq$ due to the asymmetry between the gluon and quark momentum fractions, verified with PYTHIA 8 [28], which enhances jets initiated by light valence quarks and provides sensitivity to the quark TMD FFs.

The JFFs measured using $Z$-tagged jets in this paper are defined in terms of differential cross sections $\mathrm{d}\sigma$ as

$$f(z, j_{\mathrm{T}}) = \frac{\mathrm{d}\sigma}{\mathrm{d}\mathcal{PS}\mathrm{d}z\mathrm{d}j_{\mathrm{T}}} \Big/ \frac{\mathrm{d}\sigma}{\mathrm{d}\mathcal{PS}}, \tag{2}$$

$$F(z) = \int \mathrm{d}j_{\mathrm{T}} f(z, j_{\mathrm{T}}) = \frac{\mathrm{d}\sigma}{\mathrm{d}\mathcal{PS}\mathrm{d}z} \Big/ \frac{\mathrm{d}\sigma}{\mathrm{d}\mathcal{PS}}, \tag{3}$$

$$F(j_{\mathrm{T}}) = \int \mathrm{d}z f(z, j_{\mathrm{T}}) = \frac{\mathrm{d}\sigma}{\mathrm{d}\mathcal{PS}\mathrm{d}j_{\mathrm{T}}} \Big/ \frac{\mathrm{d}\sigma}{\mathrm{d}\mathcal{PS}}, \tag{4}$$

where the phase space $\mathrm{d}\mathcal{PS}$ depends on the pseudorapidity of the $Z$ boson and the jet, and the vector sum and the difference between the transverse momenta of the $Z$ boson and the jet [13].

The TMD JFF defined in Eq. (2) is integrated over $j_{\mathrm{T}}$ to obtain the collinear JFF shown in Eq. (3). The transverse profile is obtained by integrating the TMD JFF over $z$ as defined in Eq. (4). Experimentally, these quantities can be expressed in terms of yields corrected for detector effects as

$$f(z, j_{\mathrm{T}}) = \frac{1}{N_{Z+\mathrm{jet}}} \frac{\mathrm{d}N_{\mathrm{had}}(z, j_{\mathrm{T}})}{\mathrm{d}z\mathrm{d}j_{\mathrm{T}}}, \qquad F(z) = \frac{1}{N_{Z+\mathrm{jet}}} \frac{\mathrm{d}N_{\mathrm{had}}(z)}{\mathrm{d}z},$$
$$F(j_{\mathrm{T}}) = \frac{1}{N_{Z+\mathrm{jet}}} \frac{\mathrm{d}N_{\mathrm{had}}(j_{\mathrm{T}})}{\mathrm{d}j_{\mathrm{T}}}, \tag{5}$$

where $N_{\mathrm{had}}$ is the number of hadrons in $Z$-tagged jets for given $z$ and $j_{\mathrm{T}}$, and $N_{Z+\mathrm{jet}}$ is the number of $Z+\mathrm{jet}$ pairs that contain charged hadrons.

The LHCb detector [29,30] is a single-arm forward spectrometer covering the pseudorapidity range $2 < \eta < 5$. The detector includes a high-precision tracking system consisting of a silicon-strip vertex detector (VELO) [31] surrounding the $pp$ interaction region, a silicon-strip detector located upstream of a dipole magnet with a bending power of about 4 Tm, and three stations of silicon-strip detectors and straw drift tubes [32,33] placed downstream of the magnet. The momentum resolution of charged particles provided by the tracking system is $\delta p/p \sim 0.5\%$ at low momentum and reaches 1.0% at 200 GeV.[1] The VELO allows reconstruction of multiple primary vertices (PVs) and rejection of events with more than one PV or additional low-momentum tracks. Muons are identified by a system composed of alternating layers of iron and multiwire proportional chambers [34]. Photons, electrons, and hadrons are distinguished by a calorimeter system consisting of scintillating-pad and preshower detectors, an electromagnetic calorimeter, and a hadronic calorimeter. Different types of charged hadrons are identified using information from two ring-imaging Cherenkov (RICH) detectors [35], with RICH 1 ($C_4F_{10}$ radiator) covering 2 to 60 GeV and RICH 2 ($CF_4$) covering 15 to 100 GeV. Simulated $pp$ collisions are generated using PYTHIA 8 [28] with a specific LHCb configuration [36]. Decays of hadronic particles are described by EvtGen [37], in which final-state radiation is generated using PHOTOS [38]. Finally, the Geant4 toolkit [39] is used to simulate the interactions of the particles with the detector, as described in Ref. [40].

The data sample used in this analysis corresponds to an integrated luminosity of 1.64 $\mathrm{fb}^{-1}$ collected at $\sqrt{s} =$ 13 TeV with the LHCb detector in 2016. The online event selection is performed by the muon trigger system, where $Z$ boson candidates are selected via their decay into two oppositely charged muons. The two muons are required to have $p_{\mathrm{T}} > 20$ GeV, $2.0 < \eta(\mu) < 4.5$, and their invariant mass within the range $60 < M_{\mu\mu} < 120$ GeV, as applied in Refs. [25,41]. The muons must satisfy the track-reconstruction and muon-identification criteria applied in Ref. [42]. Jet reconstruction is performed offline using a particle-flow algorithm [41], where the neutral and charged candidates are clustered using the anti-$k_T$ algorithm [43,44] with the $R$ parameter set to 0.5. The selection criteria for $Z+\mathrm{jet}$ pairs and tracks inside the jets closely follow those described in Ref. [25]. The fiducial criteria require that the jet with the highest $p_{\mathrm{T}}$ in the event, which is analyzed for these measurements, has $20 < p_{\mathrm{T}}(\mathrm{jet}) < 100$ GeV and $2.5 < \eta(\mathrm{jet}) < 4.0$. Additional jets with $p_{\mathrm{T}}(\mathrm{jet}) > 15$ GeV are used in unfolding detector effects. The tighter $\eta(\mathrm{jet})$ requirement ensures that all the jet constituents are contained within the detector acceptance. To reduce the rate of jets associated with a different primary vertex than the $Z$ candidate, only events with a single reconstructed primary vertex are analyzed. The jets must be well separated from the $Z$ candidate by requiring an azimuthal separation $\Delta\phi_{Z-\mathrm{jet}}$ greater than $\frac{7\pi}{8}$, and are rejected if one of the muons is found within $\Delta R = \sqrt{\Delta\eta^2 + \Delta\phi^2} < 0.5$, defined with respect to the jet momentum. The charged hadron candidates must be constituents of the jet, fall within $\Delta R < 0.5$ of the jet, and have a good quality track with a minimum $p_{\mathrm{T}}$ ($p$) of 0.25 (4) GeV.

[1]In this article, natural units ($c = \hbar = 1$) are used.

The number of $Z+$ jet pairs in each jet $p_{\mathrm{T}}$ interval, used in the normalization of the JFFs, is corrected to account for reconstruction and selection efficiencies. The same correction factors are applied to the hadron distributions in jets. The muon detection and reconstruction efficiencies are determined in data using the tag-and-probe method employed in the inclusive $Z$ boson cross-section measurements of LHCb [42,45,46]. The efficiency to reconstruct and identify the jet in the event is evaluated from simulation. This efficiency increases with $p_{\mathrm{T}}$, from ≈85% for jets with $p_{\mathrm{T}}$ of 20 GeV to saturate at ≈95% for jets with $p_{\mathrm{T}}$ of 30 GeV and above.

The charged hadron candidates inside the reconstructed jets are identified by the particle-identification systems [29,35]. Reconstructed charged hadron yields are corrected for the track-reconstruction efficiency, effects from misreconstructed tracks or false association with jets, and particle misidentification on a track-by-track basis. Simulation is used to determine the track reconstruction efficiency for pions, kaons, and protons separately as a function of momentum and pseudorapidity. The probability of hadronic interactions in the detector material of ≈20% $\lambda$ (nuclear interaction lengths), and decays in flight, results in track reconstruction efficiencies of 79%, 77%, and 63% for pions, kaons, and protons, respectively.

The particle identification (PID) efficiency is determined in intervals of particle momentum, pseudorapidity, and track multiplicity using dedicated data control samples [47]. The (mis)identification probabilities of charged hadrons are derived from these samples and used to construct a PID matrix. The particle misidentification effects are unfolded by solving

$$\mathbf{x}^{\mathrm{rec}} = A\mathbf{x}^{\mathrm{unf}} \tag{6}$$

in each momentum interval. The vector $\mathbf{x}^{\mathrm{unf}}$ represents the unfolded yields of the three particles species $\pi^{\pm}$, $K^{\pm}$, and $p^{\pm}$ in a given momentum interval and $\mathbf{x}^{\mathrm{rec}}$ the corresponding reconstructed yields at detector level. A matrix element $A_{ij}$ represents the probability of a particle $j$ to be reconstructed as $i$. The probabilities are weighted to describe the pseudorapidity and track-multiplicity distributions in data. Correction factors for pions (kaons) ranged from 0.98 (0.7) to 1.1 (1.03) as a function of momentum. For protons, the corrections were as large a factor of 4 at momentum below 10 GeV where PID is not fully efficient and ranged from 0.5 to 1.2 above 10 GeV. The PID corrections for kaons and protons dominate at the lowest momentum, while they compete with the track reconstruction efficiencies at higher momentum.

The uncertainties on the resulting PID-unfolded momentum distributions $\mathbf{x}^{\mathrm{unf}}$ are estimated using a bootstrap method [48] with 500 trials and are statistically dominated. The impurity of the charged-hadron sample due to misidentification of nonhadronic particles or long-lived hyperons as charged pions, kaons, or protons is less than 5% of the statistical uncertainties in all momentum intervals. The particle-species-dependent efficiencies can be biased if a particle is misidentified. The efficiencies are corrected for these effects after the PID unfolding.

The unfolding of detector effects in the distributions of transverse momentum and pseudorapidity of jets in $Z+$ jet pairs is performed using machine learning (ML) techniques based on the iterative unbinned Bayesian unfolding method as implemented in Ref. [49]. In this method, deep neural networks are employed as classifiers to estimate likelihood ratios that are used to update event weights in simulation. The unfolding method is validated with a closure test using the simulated data. In this analysis, two iterations are performed based on the best results of the closure tests. The unfolded jet-$p_{\mathrm{T}}$ distributions are consistent within statistical uncertainties between the ML method employed in this analysis and the binned iterative Bayesian method [50,51] with two iterations. The charged hadron distributions inside jets in $z$, $j_{\mathrm{T}}$, and their joint distributions, are unfolded simultaneously with the jet transverse momentum and pseudorapidity.

Sources of systematic uncertainties on the jet transverse-momentum distribution of $Z+$ jet pairs and identified charged hadrons in $z$ and $j_{\mathrm{T}}$ are evaluated. The former arise from the background contributions from fake jets (0.2%) and incorrectly reconstructed $Z$ bosons (1.4%) due to hadrons misidentified as muons. Additionally, uncertainties on the jet reconstruction are determined by comparing jet-quality quantifiers between the data and simulation (1.8%), similar to the method employed in Ref. [52]. Uncertainties related to the muon reconstruction efficiencies are found to be negligible. The $Z+$ jet selection and jet reconstruction uncertainties added in quadrature return a total uncertainty of 2.4%.

The primary uncertainties associated with the simulated detector response of the jets arise from the jet-energy scale and resolution. The jet-energy scale has been studied in previous measurements of the $Z+$ jet cross-section [41,52]. Exploiting the $p_{\mathrm{T}}$ balance between the $Z$ boson and a single recoiled jet in the event, the uncertainty on the jet-energy scale is determined to be 3%. The uncertainties on the fragmentation measurements are estimated by repeating the analysis with the energy scale in the simulation varied by one standard deviation and taking the difference in the distributions, as in Refs. [25,41,52]. Similarly, the systematic uncertainty due to the jet-energy resolution is evaluated by independently varying each component of the reconstructed jet momentum in the simulation by the uncertainty on the jet resolution. This procedure is repeated until the difference in the unfolded distributions between the nominal and smeared jet momentum stabilizes.

The sources of systematic uncertainties on the identified charged-hadron distributions include the tracking efficiency

and particle identification. The effects of the statistical precision of the efficiency are evaluated by smoothing the two-dimensional efficiency and repeating the analysis. The differences in the distributions between the smoothed and nominal efficiencies are taken as uncertainties on the tracking efficiency. Additionally, PID-dependent uncertainties attributed to the uncertainties on the material budget implemented in the simulation are found to be 1.50%, 1.27%, and 3.3% for pions, kaons, and protons, respectively. The uncertainty on the track-selection requirement to remove spurious tracks formed by accidentally matched detector hits and charged hadrons not associated with the jet is negligible. For identified charged-hadron distributions, the systematic uncertainties on the PID are determined from the uncertainties on the PID-unfolded momentum distributions.

The systematic uncertainties on the unfolding method are determined by taking the standard deviation of weighted absolute differences in the ratio between the unfolded and generated distributions. The uncertainties on the unfolded number of jets and the non-normalized hadronization variables are 1.1% and 0.8%, respectively.

Figure 1 shows $z$ and $j_{\mathrm{T}}$ distributions in three intervals of jet $p_{\mathrm{T}}$ for unidentified charged hadrons. The $z$ distributions show a humpbacked structure in $z < 0.04$ due to both color coherence and kinematic requirements. Color coherence is a manifestation of parton hadron duality [53] where the perturbative partonic structure of a jet defines the momenta of the final hadrons, and produces this structure due to the suppression of wide-angle gluon emissions. In these distributions the kinematic requirements on the tracks shift the peak of the structure to varying degrees for different jet $p_{\mathrm{T}}$ intervals; higher $p_{\mathrm{T}}$ jets can probe smaller $z$. At mid-to-high $z$, $0.04 < z < 0.4$, scaling behavior is seen across all jet $p_{\mathrm{T}}$ intervals. An overall increase of particle production in all regions of $j_{\mathrm{T}}$ for jets with higher $p_{\mathrm{T}}$ is seen, with a larger increase at high $j_{\mathrm{T}}$. Comparisons with previous measurements at $\sqrt{s} = 8$ TeV [25] show a general similarity in shape. While the measurements indicate that charged hadron production may be slightly shifted toward lower $z$ at $\sqrt{s} = 13$ TeV for a given jet $p_{\mathrm{T}}$, the $j_{\mathrm{T}}$ distributions are consistent within uncertainties between the two center-of-mass energies.

The double differential JFFs in $j_{\mathrm{T}}$, $z$, in three jet $p_{\mathrm{T}}$ intervals for unidentified charged hadrons are shown in Fig. 2. Charged hadrons carrying a larger momentum fraction along the jet axis tend to have a larger transverse momentum with respect to the jet axis. With increasing jet $p_{\mathrm{T}}$, the centroid of the joint distributions moves toward a smaller $z$, a region dominated by soft particle production, and a larger $j_{\mathrm{T}}$, resulting in wider jets. Charged particles

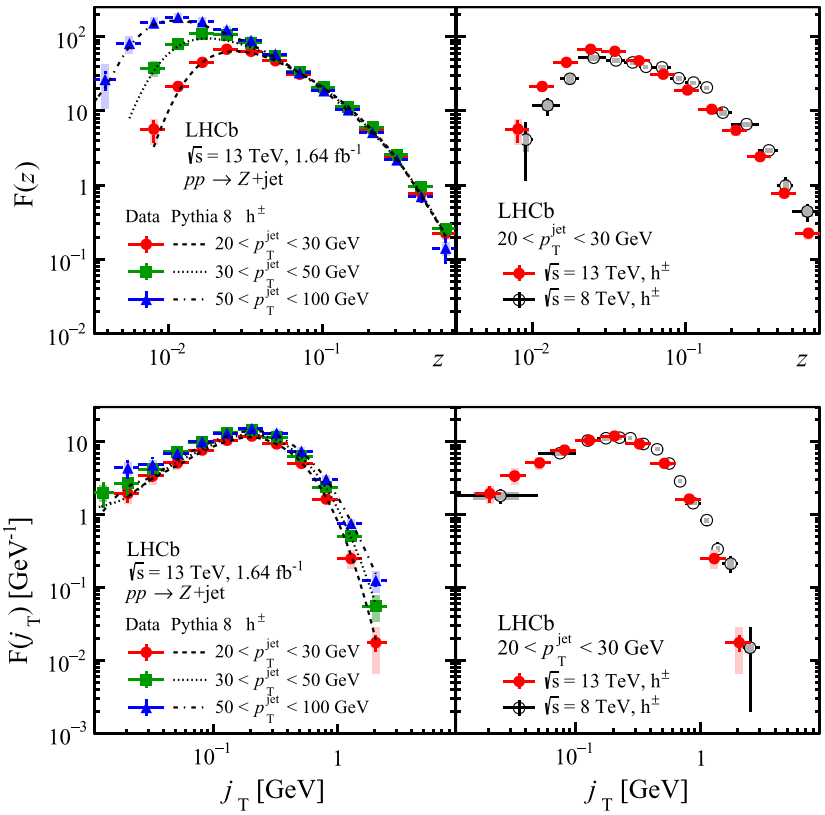


FIG. 1. Distributions of (top) the longitudinal momentum fraction and (bottom) the transverse momentum of charged hadrons (pions, kaons, and protons combined) with respect to the jet axis in three jet $p_{\mathrm{T}}$ intervals and (right) comparisons with previous results at $\sqrt{s} = 8$ TeV for jets with $20 < p_{\mathrm{T}} < 30$ GeV [25]. Statistical (systematic) uncertainties are shown in bars (boxes).

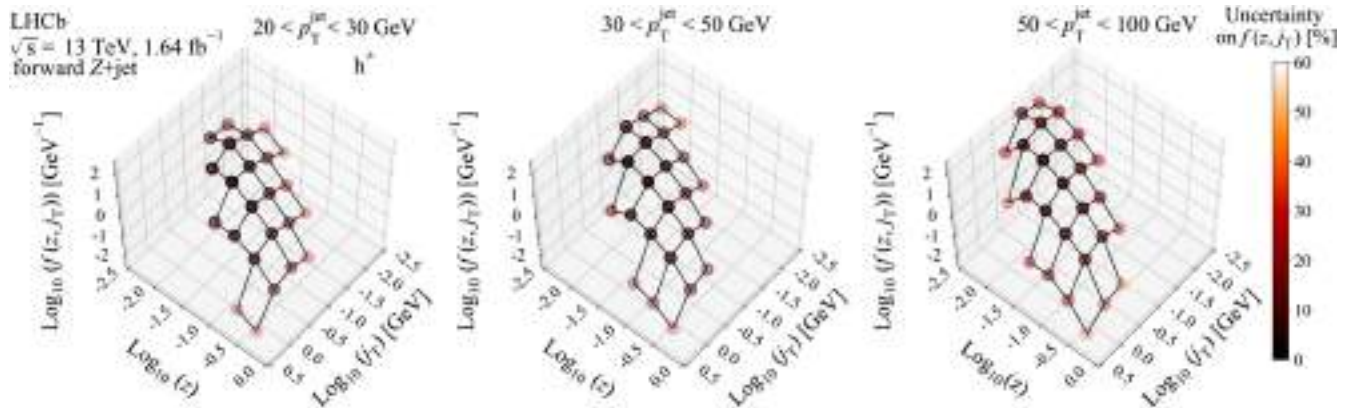


FIG. 2. Double differential JFFs of the longitudinal momentum fraction $z$ and the transverse momentum $j_T$ of charged hadrons (pions, kaons, and protons combined) in three jet $p_T$ intervals.

also carry a larger $j_T$ for a given $z$ in jets with a higher $p_T$. This is consistent with Markov chain fragmentation models, e.g., the string [5] or cluster model [6], where a momentum kick transverse to the parton system is sampled independently per hadron. Jets with higher $p_T$ experience longer Markov chains, resulting in a higher $j_T$ for a given $z$.

The $z$ distributions for identified charged hadrons and the ratios of heavier particles with respect to pions are shown in Fig. 3. Pions are the predominant charged hadron produced due to their low mass and the flavor content of the initial-state protons. Hadrons with heavier mass require a larger $z$ threshold for their formation, leading to the position of the maximum at a higher $z$. In the lowest jet $p_T$ interval, proton production relative to kaon production is clearly suppressed for lower $z$ values. When different jet $p_T$ intervals are overlaid, the scaling behavior across all jet $p_T$ intervals begins at $z \sim 0.07$ for heavier particles and 0.03 for pions.

The JFFs and the ratios are compared to predictions from PYTHIA 8 in Figs. 1 and 3. The predictions are generated using PYTHIA 8.186 with the CT09MCS PDF set and a specific LHCb configuration [36]. In general, PYTHIA 8 describes unidentified charged hadron distributions well with only slight underestimation while the number of charged pions (kaons and protons) are largely underestimated (overestimated). The production of heavier particles relative to pions is well described by PYTHIA 8 at high jet $p_T$, while at low jet $p_T$ PYTHIA 8 significantly overestimates it. These data can be used to tune MC generators for production of identified charged particles.

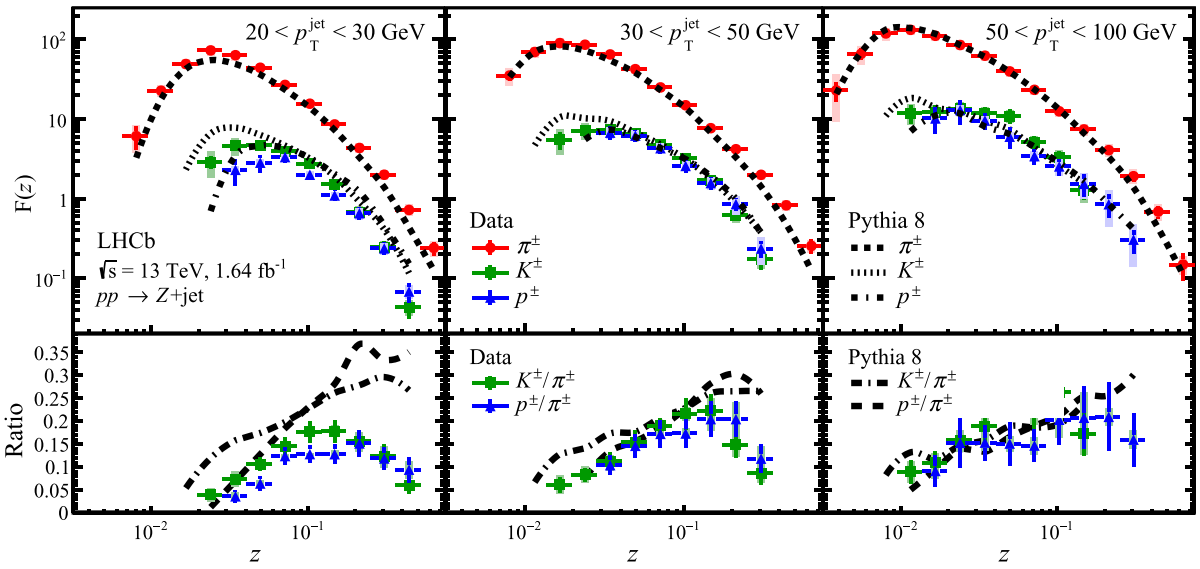


FIG. 3. Collinear jet fragmentation functions of (top) identified pions, kaons and protons in three jet $p_T$ intervals and (bottom) the ratios of kaons to pions and protons to pions. Statistical (systematic) uncertainties are shown in bars (boxes).

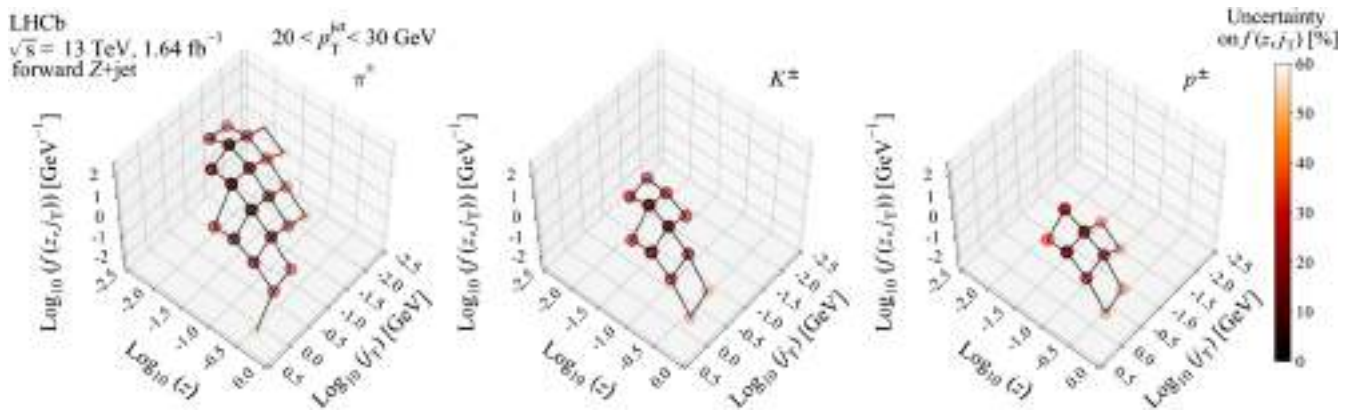


FIG. 4. Joint distributions of the longitudinal momentum fraction $z$ and the transverse momentum $j_T$ of identified charged (left) pions, (middle) kaons and (right) protons in jets with $20 < p_T < 30$ GeV.

Figure 4 shows the TMD JFFs measured as joint distributions in $z$ and $j_T$ for the three separate particle species. The center of the distribution shifting toward higher values in both $z$ and $j_T$ with the mass of the particle suggests that heavier hadrons are produced from harder partons. The results for higher jet $p_T$ intervals show this trend less clearly due to limited statistics in data [54].

In summary, the LHCb collaboration has measured the joint distributions in two kinematic variables simultaneously, probing the longitudinal and transverse profiles of identified charged pions, kaons, and protons inside predominantly light-quark-initiated jets for the first time. These distributions describe the 3D picture in the collinear and transverse dimension with respect to the jet axis, and the hadron-mass hierarchy in the hadronization processes. They will help constrain TMD FFs in uncharted phase space. These measurements exploit the full particle-identification capabilities of the LHCb detector. The joint distributions for all charged hadrons have also been measured for the first time.

The collinear JFFs for identified charged hadrons exhibit the effects of quark-flavor content inside the proton. The relative jet-fragmentation functions of heavier particles to pions could provide insights into the role of the valence versus sea quarks in the parton shower leading to hadronization. The projected single-variable distributions in $j_T$ and $z$ have been measured for identified and all charged hadrons and compared to the previous LHCb results at 8 TeV. Overall, similar patterns are seen in $j_T$ and $z > 0.04$ between $\sqrt{s} = 8$ TeV and 13 TeV.

We express our gratitude to our colleagues in the CERN accelerator departments for the excellent performance of the LHC. We thank the technical and administrative staff at the LHCb institutes. We acknowledge support from CERN and from the national agencies: CAPES, CNPq, FAPERJ and FINEP (Brazil); MOST and NSFC (China); CNRS/IN2P3 (France); BMBF, DFG and MPG (Germany); INFN (Italy); NWO (Netherlands); MNiSW and NCN (Poland); MEN/IFA (Romania); MICINN (Spain); SNSF and SER (Switzerland); NASU (Ukraine); STFC (United Kingdom); DOE NP and NSF (USA). We acknowledge the computing resources that are provided by CERN, IN2P3 (France), KIT and DESY (Germany), INFN (Italy), SURF (Netherlands), PIC (Spain), GridPP (United Kingdom), CSCS (Switzerland), IFIN-HH (Romania), CBPF (Brazil), Polish WLCG (Poland) and NERSC (USA). We are indebted to the communities behind the multiple open-source software packages on which we depend. Individual groups or members have received support from ARC and ARDC (Australia); Minciencias (Colombia); AvH Foundation (Germany); EPLANET, Marie Skłodowska-Curie Actions and ERC (European Union); A*MIDEX, ANR, IPhU and Labex P2IO, and Région Auvergne-Rhône-Alpes (France); Key Research Program of Frontier Sciences of CAS, CAS PIFI, CAS CCEPP, Fundamental Research Funds for the Central Universities, and Sci. & Tech. Program of Guangzhou (China); GVA, XuntaGal, GENCAT and Prog. Atracción Talento, CM (Spain); SRC (Sweden); the Leverhulme Trust, the Royal Society and UKRI (United Kingdom).

[1] M. Anselmino, A. Mukherjee, and A. Vossen, Transverse spin effects in hard semi-inclusive collisions, Prog. Part. Nucl. Phys. **114**, 103806 (2020).

[2] K. Kumericki, S. Liuti, and H. Moutarde, GPD phenomenology and DVCS fitting: Entering the high-precision era, Eur. Phys. J. A **52**, 157 (2016).

[3] A. Metz and A. Vossen, Parton fragmentation functions, Prog. Part. Nucl. Phys. **91**, 136 (2016).

[4] X. Artru and G. Mennessier, String model and multiproduction, Nucl. Phys. **B70**, 93 (1974).

[5] B. Andersson, G. Gustafson, G. Ingelman, and T. Sjostrand, Parton fragmentation and string dynamics, Phys. Rep. **97**, 31 (1983).

[6] G. C. Fox and S. Wolfram, A model for parton showers in QCD, Nucl. Phys. **B168**, 285 (1980).

[7] M. Procura and I. W. Stewart, Quark fragmentation within an identified jet, Phys. Rev. D **81**, 074009 (2010); **83**, 039902(E) (2011).

[8] T. Kaufmann, A. Mukherjee, and W. Vogelsang, Hadron fragmentation inside jets in hadronic collisions, Phys. Rev. D **92**, 054015 (2015); **101**, 079901(E) (2020).

[9] Y.-T. Chien, Z.-B. Kang, F. Ringer, I. Vitev, and H. Xing, Jet fragmentation functions in proton-proton collisions using soft-collinear effective theory, J. High Energy Phys. 05 (2016) 125.

[10] D. Neill, I. Scimemi, and W. J. Waalewijn, Jet axes and universal transverse-momentum-dependent fragmentation, J. High Energy Phys. 04 (2017) 020.

[11] Z.-B. Kang, F. Ringer, and I. Vitev, Jet substructure using semi-inclusive jet functions in SCET, J. High Energy Phys. 11 (2016) 155.

[12] Z.-B. Kang, X. Liu, F. Ringer, and H. Xing, The transverse momentum distribution of hadrons within jets, J. High Energy Phys. 11 (2017) 068.

[13] Z.-B. Kang, K. Lee, J. Terry, and H. Xing, Jet fragmentation functions for Z-tagged jets, Phys. Lett. B **798**, 134978 (2019).

[14] J. Collins, *Foundations of Perturbative QCD* (Cambridge University Press, Cambridge, England, 2013), Vol. 32.

[15] K. Abe *et al.* (Belle Collaboration), Measurement of Azimuthal Asymmetries in Inclusive Production of Hadron Pairs in $e^+e^-$ Annihilation at Belle, Phys. Rev. Lett. **96**, 232002 (2006).

[16] R. Seidl *et al.* (Belle Collaboration), Measurement of azimuthal asymmetries in inclusive production of hadron pairs in $e^+e^-$ annihilation at $\sqrt{s} = 10.58$ GeV, Phys. Rev. D **78**, 032011 (2008); **86**, 039905(E) (2012).

[17] J. P. Lees *et al.* (*BABAR* Collaboration), Measurement of Collins asymmetries in inclusive production of charged pion pairs in $e^+e^-$ annihilation at *BABAR*, Phys. Rev. D **90**, 052003 (2014).

[18] R. Seidl *et al.* (Belle Collaboration), Transverse momentum dependent production cross sections of charged pions, kaons and protons produced in inclusive $e^+e^-$ annihilation at $\sqrt{s} = 10.58$ GeV, Phys. Rev. D **99**, 112006 (2019).

[19] J. P. Lees *et al.* (*BABAR* Collaboration), Collins asymmetries in inclusive charged $KK$ and $K\pi$ pairs produced in $e^+e^-$ annihilation, Phys. Rev. D **92**, 111101 (2015).

[20] M. Ablikim *et al.* (BESIII Collaboration), Measurement of Azimuthal Asymmetries in Inclusive Charged Dipion Production in $e^+e^-$ Annihilations at $\sqrt{s} = 3.65$ GeV, Phys. Rev. Lett. **116**, 042001 (2016).

[21] A. Airapetian *et al.* (HERMES Collaboration), Multiplicities of charged pions and kaons from semi-inclusive deep-inelastic scattering by the proton and the deuteron, Phys. Rev. D **87**, 074029 (2013).

[22] M. Aghasyan *et al.* (COMPASS Collaboration), Transverse-momentum-dependent multiplicities of charged hadrons in muon-deuteron deep inelastic scattering, Phys. Rev. D **97**, 032006 (2018).

[23] G. Aad *et al.* (ATLAS Collaboration), Measurement of the jet fragmentation function and transverse profile in proton-proton collisions at a center-of-mass energy of 7 TeV with the ATLAS detector, Eur. Phys. J. C **71**, 1795 (2011).

[24] G. Aad *et al.* (ATLAS Collaboration), Properties of jet fragmentation using charged particles measured with the ATLAS detector in $pp$ collisions at $\sqrt{s} = 13$ TeV, Phys. Rev. D **100**, 052011 (2019).

[25] R. Aaij *et al.* (LHCb Collaboration), Measurement of Charged Hadron Production in $Z$-Tagged Jets in Proton-Proton Collisions at $\sqrt{s} = 8$ TeV, Phys. Rev. Lett. **123**, 232001 (2019).

[26] S. Acharya *et al.* (ALICE Collaboration), Jet fragmentation transverse momentum distributions in pp and p-Pb collisions at $\sqrt{s}$, $\sqrt{s_{\mathrm{NN}}} = 5.02$ TeV, J. High Energy Phys. 09 (2021) 211.

[27] L. Adamczyk *et al.* (STAR Collaboration), Azimuthal transverse single-spin asymmetries of inclusive jets and charged pions within jets from polarized-proton collisions at $\sqrt{s} = 500$ GeV, Phys. Rev. D **97**, 032004 (2018).

[28] T. Sjöstrand, S. Mrenna, and P. Skands, A brief introduction to PYTHIA 8.1, Comput. Phys. Commun. **178**, 852 (2008); PYTHIA 6.4 physics and manual, J. High Energy Phys. 05 (2006) 026.

[29] A. A. Alves, Jr. *et al.* (LHCb Collaboration), The LHCb detector at the LHC, J. Instrum. **3**, S08005 (2008).

[30] LHCb Collaboration, LHCb detector performance, Int. J. Mod. Phys. A **30**, 1530022 (2015).

[31] R. Aaij *et al.*, Performance of the LHCb vertex locator, J. Instrum. **9**, P09007 (2014).

[32] R. Arink *et al.*, Performance of the LHCb outer tracker, J. Instrum. **9**, P01002 (2014).

[33] P. d'Argent *et al.*, Improved performance of the LHCb outer tracker in LHC Run 2, J. Instrum. **12**, P11016 (2017).

[34] A. A. Alves, Jr. *et al.*, Performance of the LHCb muon system, J. Instrum. **8**, P02022 (2013).

[35] M. Adinolfi *et al.*, Performance of the LHCb RICH detector at the LHC, Eur. Phys. J. C **73**, 2431 (2013).

[36] I. Belyaev *et al.*, Handling of the generation of primary events in Gauss, the LHCb simulation framework, J. Phys. Conf. Ser. **331**, 032047 (2011).

[37] D. J. Lange, The EvtGen particle decay simulation package, Nucl. Instrum. Methods Phys. Res., Sect. A **462**, 152 (2001).

[38] N. Davidson, T. Przedzinski, and Z. Was, PHOTOS interface in C++: Technical and physics documentation, Comput. Phys. Commun. **199**, 86 (2016).

[39] S. Agostinelli *et al.* (Geant4 Collaboration), Geant4: A simulation toolkit, Nucl. Instrum. Methods Phys. Res., Sect. A **506**, 250 (2003); J. Allison *et al.* (Geant4 Collaboration), Geant4 developments and applications, IEEE Trans. Nucl. Sci. **53**, 270 (2006).

[40] M. Clemencic, G. Corti, S. Easo, C. R. Jones, S. Miglioranzi, M. Pappagallo, and P. Robbe, The LHCb simulation application, Gauss: Design, evolution and experience, J. Phys. Conf. Ser. **331**, 032023 (2011).

[41] R. Aaij *et al.* (LHCb Collaboration), Study of forward $Z+$ jet production in $pp$ collisions at $\sqrt{s}=7$ TeV, J. High Energy Phys. 01 (2014) 033.
[42] R. Aaij *et al.* (LHCb Collaboration), Precision measurement of forward $Z$ boson production in proton-proton collisions at $\sqrt{s}=13$ TeV, J. High Energy Phys. 07 (2022) 026.
[43] M. Cacciari, G. P. Salam, and G. Soyez, The anti-$k_t$ jet clustering algorithm, J. High Energy Phys. 04 (2008) 063.
[44] M. Cacciari, G. P. Salam, and G. Soyez, FastJet user manual, Eur. Phys. J. C **72**, 1896 (2012).
[45] R. Aaij *et al.* (LHCb Collaboration), Measurement of forward $W$ and $Z$ boson production in $pp$ collisions at $\sqrt{s}=8$ TeV, J. High Energy Phys. 01 (2016) 155.
[46] R. Aaij *et al.* (LHCb Collaboration), Measurement of the forward $Z$ boson production cross-section in $pp$ collisions at $\sqrt{s}=7$ TeV, J. High Energy Phys. 08 (2015) 039.
[47] L. Anderlini *et al.*, The PIDCalib package, Report No. LHCb-PUB-2016-021, 2016, https://cds.cern.ch/record/2202412.
[48] B. Efron, Bootstrap methods: Another look at the jackknife, Ann. Stat. **7**, 1 (1979).
[49] A. Andreassen, P. T. Komiske, E. M. Metodiev, B. Nachman, and J. Thaler, OmniFold: A Method to Simultaneously Unfold all Observables, Phys. Rev. Lett. **124**, 182001 (2020).
[50] G. D'Agostini, A multidimensional unfolding method based on Bayes' theorem, Nucl. Instrum. Methods Phys. Res., Sect. A **362**, 487 (1995).
[51] T. Adye, Unfolding algorithms and tests using RooUnfold, in *PHYSTAT 2011* (CERN, Geneva, 2011), pp. 313–318.
[52] R. Aaij *et al.* (LHCb Collaboration), Measurement of forward $W$ and $Z$ boson production in association with jets in proton-proton collisions at $\sqrt{s}=8$ TeV, J. High Energy Phys. 05 (2016) 131.
[53] Y. I. Azimov, Y. L. Dokshitzer, V. A. Khoze, and S. I. Troyan, Humpbacked QCD plateau in hadron spectra, Z. Phys. C **31**, 213 (1986).
[54] See Supplemental Material at http://link.aps.org/supplemental/10.1103/PhysRevD.108.L031103 for further details.

R. Aaij,[32] A. S. W. Abdelmotteleb,[50] C. Abellan Beteta,[44] F. Abudinén,[50] T. Ackernley,[54] B. Adeva,[40] M. Adinolfi,[48] H. Afsharnia,[9] C. Agapopoulou,[13] C. A. Aidala,[76] S. Aiola,[25] Z. Ajaltouni,[9] S. Akar,[59] K. Akiba,[32] J. Albrecht,[15] F. Alessio,[42] M. Alexander,[53] A. Alfonso Albero,[39] Z. Aliouche,[56] P. Alvarez Cartelle,[49] R. Amalric,[13] S. Amato,[2] J. L. Amey,[48] Y. Amhis,[11,42] L. An,[42] L. Anderlini,[22] M. Andersson,[44] A. Andreianov,[38] M. Andreotti,[21] D. Andreou,[62] D. Ao,[6] F. Archilli,[17] A. Artamonov,[38] M. Artuso,[62] E. Aslanides,[10] M. Atzeni,[44] B. Audurier,[12] S. Bachmann,[17] M. Bachmayer,[43] J. J. Back,[50] A. Bailly-reyre,[13] P. Baladron Rodriguez,[40] V. Balagura,[12] W. Baldini,[21] J. Baptista de Souza Leite,[1] M. Barbetti,[22,b] R. J. Barlow,[56] S. Barsuk,[11] W. Barter,[55] M. Bartolini,[49] F. Baryshnikov,[38] J. M. Basels,[14] G. Bassi,[29,c] B. Batsukh,[4] A. Battig,[15] A. Bay,[43] A. Beck,[50] M. Becker,[15] F. Bedeschi,[29] I. B. Bediaga,[1] A. Beiter,[62] V. Belavin,[38] S. Belin,[40] V. Bellee,[44] K. Belous,[38] I. Belov,[38] I. Belyaev,[38] G. Benane,[10] G. Bencivenni,[23] E. Ben-Haim,[13] A. Berezhnoy,[38] R. Bernet,[44] D. Berninghoff,[17] H. C. Bernstein,[62] C. Bertella,[56] A. Bertolin,[28] C. Betancourt,[44] F. Betti,[42] Ia. Bezshyiko,[44] S. Bhasin,[48] J. Bhom,[35] L. Bian,[67] M. S. Bieker,[15] N. V. Biesuz,[21] S. Bifani,[47] P. Billoir,[13] A. Biolchini,[32] M. Birch,[55] F. C. R. Bishop,[49] A. Bitadze,[56] A. Bizzeti, M. P. Blago,[49] T. Blake,[50] F. Blanc,[43] S. Blusk,[62] D. Bobulska,[53] J. A. Boelhauve,[15] O. Boente Garcia,[12] T. Boettcher,[59] A. Boldyrev,[38] C. S. Bolognani,[73] N. Bondar,[38,42] S. Borghi,[56] M. Borsato,[17] J. T. Borsuk,[35] S. A. Bouchiba,[43] T. J. V. Bowcock,[54,42] A. Boyer,[42] C. Bozzi,[21] M. J. Bradley,[55] S. Braun,[60] A. Brea Rodriguez,[40] J. Brodzicka,[35] A. Brossa Gonzalo,[50] D. Brundu,[27] A. Buonaura,[44] L. Buonincontri,[28] A. T. Burke,[56] C. Burr,[42] A. Bursche,[66] A. Butkevich,[38] J. S. Butter,[32] J. Buytaert,[42] W. Byczynski,[42] S. Cadeddu,[27] H. Cai,[67] R. Calabrese,[21,d] L. Calefice,[15,13] S. Cali,[23] R. Calladine,[47] M. Calvi,[26,e] M. Calvo Gomez,[74] P. Campana,[23] D. H. Campora Perez,[73] A. F. Campoverde Quezada,[6] S. Capelli,[26,e] L. Capriotti,[20,f] A. Carbone,[20,f] G. Carboni,[31] R. Cardinale,[24,g] A. Cardini,[27] I. Carli,[4] P. Carniti,[26,e] L. Carus,[14] A. Casais Vidal,[40] R. Caspary,[17] G. Casse,[54] M. Cattaneo,[42] G. Cavallero,[42] V. Cavallini,[21,d] S. Celani,[43] J. Cerasoli,[10] D. Cervenkov,[57] A. J. Chadwick,[54] M. G. Chapman,[48] M. Charles,[13] Ph. Charpentier,[42] C. A. Chavez Barajas,[54] M. Chefdeville,[8] C. Chen,[3] S. Chen,[4] A. Chernov,[35] S. Chernyshenko,[46] V. Chobanova,[40] S. Cholak,[43] M. Chrzaszcz,[35] A. Chubykin,[38] V. Chulikov,[38] P. Ciambrone,[23] M. F. Cicala,[50] X. Cid Vidal,[40] G. Ciezarek,[42] G. Ciullo,[21,d] P. E. L. Clarke,[52] M. Clemencic,[42] H. V. Cliff,[49] J. Closier,[42] J. L. Cobbledick,[56] V. Coco,[42] J. A. B. Coelho,[11] J. Cogan,[10] E. Cogneras,[9] L. Cojocariu,[37] P. Collins,[42] T. Colombo,[42] L. Congedo,[19] A. Contu,[27] N. Cooke,[47] G. Coombs,[53] I. Corredoira,[40] G. Corti,[42] B. Couturier,[42] D. C. Craik,[58] J. Crkovská,[61] M. Cruz Torres,[1,h] R. Currie,[52] C. L. Da Silva,[61] S. Dadabaev,[38] L. Dai,[65] X. Dai,[5] E. Dall'Occo,[15] J. Dalseno,[40] C. D'Ambrosio,[42] A. Danilina,[38] P. d'Argent,[15] J. E. Davies,[56] A. Davis,[56] O. De Aguiar Francisco,[56]

J. de Boer,[42] K. De Bruyn,[72] S. De Capua,[56] M. De Cian,[43] U. De Freitas Carneiro Da Graca,[1] E. De Lucia,[23] J. M. De Miranda,[1] L. De Paula,[2] M. De Serio,[19,i] D. De Simone,[44] P. De Simone,[23] F. De Vellis,[15] J. A. de Vries,[73] C. T. Dean,[61] F. Debernardis,[19,i] D. Decamp,[8] V. Dedu,[10] L. Del Buono,[13] B. Delaney,[58] H.-P. Dembinski,[15] V. Denysenko,[44] O. Deschamps,[9] F. Dettori,[27,j] B. Dey,[70] A. Di Cicco,[23] P. Di Nezza,[23] I. Diachkov,[38] S. Didenko,[38] L. Dieste Maronas,[40] S. Ding,[62] V. Dobishuk,[46] A. Dolmatov,[38] C. Dong,[3] A. M. Donohoe,[18] F. Dordei,[27] A. C. dos Reis,[1] L. Douglas,[53] A. G. Downes,[8] M. W. Dudek,[35] L. Dufour,[42] V. Duk,[71] P. Durante,[42] J. M. Durham,[61] D. Dutta,[56] A. Dziurda,[35] A. Dzyuba,[38] S. Easo,[51] U. Egede,[63] V. Egorychev,[38] S. Eidelman,[38,a] C. Eirea Orro,[40] S. Eisenhardt,[52] S. Ek-In,[43] L. Eklund,[75] S. Ely,[62] A. Ene,[37] E. Epple,[61] S. Escher,[14] J. Eschle,[44] S. Esen,[44] T. Evans,[56] L. N. Falcao,[1] Y. Fan,[6] B. Fang,[67] S. Farry,[54] D. Fazzini,[26,e] M. Feo,[42] A. D. Fernez,[60] F. Ferrari,[20] L. Ferreira Lopes,[43] F. Ferreira Rodrigues,[2] S. Ferreres Sole,[32] M. Ferrillo,[44] M. Ferro-Luzzi,[42] S. Filippov,[38] R. A. Fini,[19] M. Fiorini,[21,d] M. Firlej,[34] K. M. Fischer,[57] D. S. Fitzgerald,[76] C. Fitzpatrick,[56] T. Fiutowski,[34] F. Fleuret,[12] M. Fontana,[13] F. Fontanelli,[24,g] R. Forty,[42] D. Foulds-Holt,[49] V. Franco Lima,[54] M. Franco Sevilla,[60] M. Frank,[42] E. Franzoso,[21,d] G. Frau,[17] C. Frei,[42] D. A. Friday,[53] J. Fu,[6] Q. Fuehring,[15] E. Gabriel,[32] G. Galati,[19,i] M. D. Galati,[72] A. Gallas Torreira,[40] D. Galli,[20,f] S. Gambetta,[52,42] Y. Gan,[3] M. Gandelman,[2] P. Gandini,[25] Y. Gao,[5] M. Garau,[27,j] L. M. Garcia Martin,[50] P. Garcia Moreno,[39] J. García Pardiñas,[26,e] B. Garcia Plana,[40] F. A. Garcia Rosales,[12] L. Garrido,[39] C. Gaspar,[42] R. E. Geertsema,[32] D. Gerick,[17] L. L. Gerken,[15] E. Gersabeck,[56] M. Gersabeck,[56] T. Gershon,[50] L. Giambastiani,[28] V. Gibson,[49] H. K. Giemza,[36] A. L. Gilman,[57] M. Giovannetti,[23,k] A. Gioventù,[40] P. Gironella Gironell,[39] C. Giugliano,[21,d] M. A. Giza,[35] K. Gizdov,[52] E. L. Gkougkousis,[42] V. V. Gligorov,[13,42] C. Göbel,[64] E. Golobardes,[74] D. Golubkov,[38] A. Golutvin,[55,38] A. Gomes,[1,l] S. Gomez Fernandez,[39] F. Goncalves Abrantes,[57] M. Goncerz,[35] G. Gong,[3] I. V. Gorelov,[38] C. Gotti,[26] J. P. Grabowski,[17] T. Grammatico,[13] L. A. Granado Cardoso,[42] E. Graugés,[39] E. Graverini,[43] G. Graziani, A. T. Grecu,[37] L. M. Greeven,[32] N. A. Grieser,[4] L. Grillo,[53] S. Gromov,[38] B. R. Gruberg Cazon,[57] C. Gu,[3] M. Guarise,[21,d] M. Guittiere,[11] P. A. Günther,[17] E. Gushchin,[38] A. Guth,[14] Y. Guz,[38] T. Gys,[42] T. Hadavizadeh,[63] G. Haefeli,[43] C. Haen,[42] J. Haimberger,[42] S. C. Haines,[49] T. Halewood-leagas,[54] M. M. Halvorsen,[42] P. M. Hamilton,[60] J. Hammerich,[54] Q. Han,[7] X. Han,[17] E. B. Hansen,[56] S. Hansmann-Menzemer,[17,42] L. Hao,[6] N. Harnew,[57] T. Harrison,[54] C. Hasse,[42] M. Hatch,[42] J. He,[6,m] K. Heijhoff,[32] K. Heinicke,[15] C. Henderson,[59] R. D. L. Henderson,[63,50] A. M. Hennequin,[58] K. Hennessy,[54] L. Henry,[42] J. Heuel,[14] A. Hicheur,[2] D. Hill,[43] M. Hilton,[56] S. E. Hollitt,[15] R. Hou,[7] Y. Hou,[8] J. Hu,[17] J. Hu,[66] W. Hu,[5] X. Hu,[3] W. Huang,[6] X. Huang,[67] W. Hulsbergen,[32] R. J. Hunter,[50] M. Hushchyn,[38] D. Hutchcroft,[54] P. Ibis,[15] M. Idzik,[34] D. Ilin,[38] P. Ilten,[59] A. Inglessi,[38] A. Iniukhin,[38] A. Ishteev,[38] K. Ivshin,[38] R. Jacobsson,[42] H. Jage,[14] S. J. Jaimes Elles,[41] S. Jakobsen,[42] E. Jans,[32] B. K. Jashal,[41] A. Jawahery,[60] V. Jevtic,[15] X. Jiang,[4,6] Y. Jiang,[6] M. John,[57] D. Johnson,[58] C. R. Jones,[49] T. P. Jones,[50] B. Jost,[42] N. Jurik,[42] I. Juszczak,[35] S. Kandybei,[45] Y. Kang,[3] M. Karacson,[42] D. Karpenkov,[38] M. Karpov,[38] J. W. Kautz,[59] F. Keizer,[42] D. M. Keller,[62] M. Kenzie,[50] T. Ketel,[33] B. Khanji,[15] A. Kharisova,[38] S. Kholodenko,[38] T. Kirn,[14] V. S. Kirsebom,[43] O. Kitouni,[58] S. Klaver,[33] N. Kleijne,[29,c] K. Klimaszewski,[36] M. R. Kmiec,[36] S. Koliiev,[46] A. Kondybayeva,[38] A. Konoplyannikov,[38] P. Kopciewicz,[34] R. Kopecna,[17] P. Koppenburg,[32] M. Korolev,[38] I. Kostiuk,[32,46] O. Kot,[46] S. Kotriakhova, A. Kozachuk,[38] P. Kravchenko,[38] L. Kravchuk,[38] R. D. Krawczyk,[42] M. Kreps,[50] S. Kretzschmar,[14] P. Krokovny,[38] W. Krupa,[34] W. Krzemien,[36] J. Kubat,[17] W. Kucewicz,[35,34] M. Kucharczyk,[35] V. Kudryavtsev,[38] G. J. Kunde,[61] A. Kupsc,[75] D. Lacarrere,[42] G. Lafferty,[56] A. Lai,[27] A. Lampis,[27,j] D. Lancierini,[44] C. Landesa Gomez,[40] J. J. Lane,[56] R. Lane,[48] G. Lanfranchi,[23] C. Langenbruch,[14] J. Langer,[15] O. Lantwin,[38] T. Latham,[50] F. Lazzari,[29,n] M. Lazzaroni,[25,o] R. Le Gac,[10] S. H. Lee,[76] R. Lefèvre,[9] A. Leflat,[38] S. Legotin,[38] P. Lenisa,[21,d] O. Leroy,[10] T. Lesiak,[35] B. Leverington,[17] A. Li,[3] H. Li,[66] K. Li,[7] P. Li,[17] S. Li,[7] T. Li,[66] Y. Li,[4] Z. Li,[62] X. Liang,[62] C. Lin,[6] T. Lin,[51] R. Lindner,[42] V. Lisovskyi,[15] R. Litvinov,[27,j] G. Liu,[66] H. Liu,[6] Q. Liu,[6] S. Liu,[4,6] A. Lobo Salvia,[39] A. Loi,[27] R. Lollini,[71] J. Lomba Castro,[40] I. Longstaff,[53] J. H. Lopes,[2] S. López Soliño,[40] G. H. Lovell,[49] Y. Lu,[4,p] C. Lucarelli,[22,b] D. Lucchesi,[28,q] S. Luchuk,[38] M. Lucio Martinez,[32] V. Lukashenko,[32,46] Y. Luo,[3] A. Lupato,[56] E. Luppi,[21,d] A. Lusiani,[29,c] K. Lynch,[18] X.-R. Lyu,[6] L. Ma,[4] R. Ma,[6] S. Maccolini,[20] F. Machefert,[11] F. Maciuc,[37] V. Macko,[43] P. Mackowiak,[15] S. Maddrell-Mander,[48] L. R. Madhan Mohan,[48] A. Maevskiy,[38] D. Maisuzenko,[38] M. W. Majewski,[34]

J. J. Malczewski,[35] S. Malde,[57] B. Malecki,[35,42] A. Malinin,[38] T. Maltsev,[38] H. Malygina,[17] G. Manca,[27,j] G. Mancinelli,[10] D. Manuzzi,[20] C. A. Manzari,[44] D. Marangotto,[25,o] J. F. Marchand,[8] U. Marconi,[20] S. Mariani,[22,b] C. Marin Benito,[39] M. Marinangeli,[43] J. Marks,[17] A. M. Marshall,[48] P. J. Marshall,[54] G. Martelli,[71,r] G. Martellotti,[30] L. Martinazzoli,[42,e] M. Martinelli,[26,e] D. Martinez Santos,[40] F. Martinez Vidal,[41] A. Massafferri,[1] M. Materok,[14] R. Matev,[42] A. Mathad,[44] V. Matiunin,[38] C. Matteuzzi,[26] K. R. Mattioli,[76] A. Mauri,[32] E. Maurice,[12] J. Mauricio,[39] M. Mazurek,[42] M. McCann,[55] L. Mcconnell,[18] T. H. McGrath,[56] N. T. McHugh,[53] A. McNab,[56] R. McNulty,[18] J. V. Mead,[54] B. Meadows,[59] G. Meier,[15] D. Melnychuk,[36] S. Meloni,[26,e] M. Merk,[32,73] A. Merli,[25,o] L. Meyer Garcia,[2] D. Miao,[4,6] M. Mikhasenko,[69,s] D. A. Milanes,[68] E. Millard,[50] M. Milovanovic,[42] M.-N. Minard,[8,a] A. Minotti,[26,e] S. E. Mitchell,[52] B. Mitreska,[56] D. S. Mitzel,[15] A. Mödden,[15] R. A. Mohammed,[57] R. D. Moise,[14] S. Mokhnenko,[38] T. Mombächer,[40] I. A. Monroy,[68] S. Monteil,[9] M. Morandin,[28] G. Morello,[23] M. J. Morello,[29,c] J. Moron,[34] A. B. Morris,[69] A. G. Morris,[50] R. Mountain,[62] H. Mu,[3] F. Muheim,[52] M. Mulder,[72] K. Müller,[44] C. H. Murphy,[57] D. Murray,[56] R. Murta,[55] P. Muzzetto,[27,j] P. Naik,[48] T. Nakada,[43] R. Nandakumar,[51] T. Nanut,[42] I. Nasteva,[2] M. Needham,[52] N. Neri,[25,o] S. Neubert,[69] N. Neufeld,[42] P. Neustroev,[38] R. Newcombe,[55] E. M. Niel,[43] S. Nieswand,[14] N. Nikitin,[38] N. S. Nolte,[58] C. Normand,[8,27,j] J. Novoa Fernandez,[40] C. Nunez,[76] A. Oblakowska-Mucha,[34] V. Obraztsov,[38] T. Oeser,[14] D. P. O'Hanlon,[48] S. Okamura,[21,d] R. Oldeman,[27,j] F. Oliva,[52] M. E. Olivares,[62] C. J. G. Onderwater,[72] R. H. O'Neil,[52] J. M. Otalora Goicochea,[2] T. Ovsiannikova,[38] P. Owen,[44] A. Oyanguren,[41] O. Ozcelik,[52] K. O. Padeken,[69] B. Pagare,[50] P. R. Pais,[42] T. Pajero,[57] A. Palano,[19] M. Palutan,[23] Y. Pan,[56] G. Panshin,[38] A. Papanestis,[51] M. Pappagallo,[19,i] L. L. Pappalardo,[21,d] C. Pappenheimer,[59] W. Parker,[60] C. Parkes,[56] B. Passalacqua,[21,d] G. Passaleva,[22] A. Pastore,[19] M. Patel,[55] C. Patrignani,[20,f] C. J. Pawley,[73] A. Pearce,[42] A. Pellegrino,[32] M. Pepe Altarelli,[42] S. Perazzini,[20] D. Pereima,[38] A. Pereiro Castro,[40] P. Perret,[9] M. Petric,[53] K. Petridis,[48] A. Petrolini,[24,g] A. Petrov,[38] S. Petrucci,[52] M. Petruzzo,[25] H. Pham,[62] A. Philippov,[38] R. Piandani,[6] L. Pica,[29,c] M. Piccini,[71] B. Pietrzyk,[8] G. Pietrzyk,[11] M. Pili,[57] D. Pinci,[30] F. Pisani,[42] M. Pizzichemi,[26,42,e] V. Placinta,[37] J. Plews,[47] M. Plo Casasus,[40] F. Polci,[13,42] M. Poli Lener,[23] M. Poliakova,[62] A. Poluektov,[10] N. Polukhina,[38] I. Polyakov,[42] E. Polycarpo,[2] S. Ponce,[42] D. Popov,[6,42] S. Popov,[38] S. Poslavskii,[38] K. Prasanth,[35] L. Promberger,[42] C. Prouve,[40] V. Pugatch,[46] V. Puill,[11] G. Punzi,[29,t] H. R. Qi,[3] W. Qian,[6] N. Qin,[3] S. Qu,[3] R. Quagliani,[43] N. V. Raab,[18] R. I. Rabadan Trejo,[6] B. Rachwal,[34] J. H. Rademacker,[48] R. Rajagopalan,[62] M. Rama,[29] M. Ramos Pernas,[50] M. S. Rangel,[2] F. Ratnikov,[38] G. Raven,[33,42] M. Rebollo De Miguel,[41] F. Redi,[42] F. Reiss,[56] C. Remon Alepuz,[41] Z. Ren,[3] V. Renaudin,[57] P. K. Resmi,[10] R. Ribatti,[29,c] A. M. Ricci,[27] S. Ricciardi,[51] K. Richardson,[58] M. Richardson-Slipper,[52] K. Rinnert,[54] P. Robbe,[11] G. Robertson,[52] A. B. Rodrigues,[43] E. Rodrigues,[54] J. A. Rodriguez Lopez,[68] E. Rodriguez Rodriguez,[40] A. Rollings,[57] P. Roloff,[42] V. Romanovskiy,[38] M. Romero Lamas,[40] A. Romero Vidal,[40] J. D. Roth,[76,a] M. Rotondo,[23] M. S. Rudolph,[62] T. Ruf,[42] R. A. Ruiz Fernandez,[40] J. Ruiz Vidal,[41] A. Ryzhikov,[38] J. Ryzka,[34] J. J. Saborido Silva,[40] N. Sagidova,[38] N. Sahoo,[47] B. Saitta,[27,j] M. Salomoni,[42] C. Sanchez Gras,[32] I. Sanderswood,[41] R. Santacesaria,[30] C. Santamarina Rios,[40] M. Santimaria,[23] E. Santovetti,[31,k] D. Saranin,[38] G. Sarpis,[14] M. Sarpis,[69] A. Sarti,[30] C. Satriano,[30,u] A. Satta,[31] M. Saur,[15] D. Savrina,[38] H. Sazak,[9] L. G. Scantlebury Smead,[57] A. Scarabotto,[13] S. Schael,[14] S. Scherl,[54] M. Schiller,[53] H. Schindler,[42] M. Schmelling,[16] B. Schmidt,[42] S. Schmitt,[14] O. Schneider,[43] A. Schopper,[42] M. Schubiger,[32] S. Schulte,[43] M. H. Schune,[11] R. Schwemmer,[42] B. Sciascia,[23,42] A. Sciuccati,[42] S. Sellam,[40] A. Semennikov,[38] M. Senghi Soares,[33] A. Sergi,[24,g] N. Serra,[44] L. Sestini,[28] A. Seuthe,[15] Y. Shang,[5] D. M. Shangase,[76] M. Shapkin,[38] I. Shchemerov,[38] L. Shchutska,[43] T. Shears,[54] L. Shekhtman,[38] Z. Shen,[5] S. Sheng,[4,6] V. Shevchenko,[38] B. Shi,[6] E. B. Shields,[26,e] Y. Shimizu,[11] E. Shmanin,[38] J. D. Shupperd,[62] B. G. Siddi,[21,d] R. Silva Coutinho,[44] G. Simi,[28] S. Simone,[19,i] M. Singla,[63] N. Skidmore,[56] R. Skuza,[17] T. Skwarnicki,[62] M. W. Slater,[47] J. C. Smallwood,[57] J. G. Smeaton,[49] E. Smith,[44] K. Smith,[61] M. Smith,[55] A. Snoch,[32] L. Soares Lavra,[9] M. D. Sokoloff,[59] F. J. P. Soler,[53] A. Solomin,[38,48] A. Solovev,[38] I. Solovyev,[38] F. L. Souza De Almeida,[2] B. Souza De Paula,[2] B. Spaan,[15,a] E. Spadaro Norella,[25,o] E. Spiridenkov,[38] P. Spradlin,[53] V. Sriskaran,[42] F. Stagni,[42] M. Stahl,[59] S. Stahl,[42] S. Stanislaus,[57] E. N. Stein,[42] O. Steinkamp,[44] O. Stenyakin,[38] H. Stevens,[15] S. Stone,[62,a] D. Strekalina,[38] F. Suljik,[57] J. Sun,[27] L. Sun,[67] Y. Sun,[60] P. Svihra,[56] P. N. Swallow,[47] K. Swientek,[34] A. Szabelski,[36] T. Szumlak,[34] M. Szymanski,[42] Y. Tan,[3] S. Taneja,[56]

A. R. Tanner,[48] M. D. Tat,[57] A. Terentev,[38] F. Teubert,[42] E. Thomas,[42] D. J. D. Thompson,[47] K. A. Thomson,[54] H. Tilquin,[55] V. Tisserand,[9] S. T'Jampens,[8] M. Tobin,[4] L. Tomassetti,[21,d] G. Tonani,[25,o] X. Tong,[5] D. Torres Machado,[1] D. Y. Tou,[3] E. Trifonova,[38] S. M. Trilov,[48] C. Trippl,[43] G. Tuci,[6] A. Tully,[43] N. Tuning,[32,42] A. Ukleja,[36] D. J. Unverzagt,[17] E. Ursov,[38] A. Usachov,[32] A. Ustyuzhanin,[38] U. Uwer,[17] A. Vagner,[38] V. Vagnoni,[20] A. Valassi,[42] G. Valenti,[20] N. Valls Canudas,[74] M. van Beuzekom,[32] M. Van Dijk,[43] H. Van Hecke,[61] E. van Herwijnen,[38] C. B. Van Hulse,[40] M. van Veghel,[72] R. Vazquez Gomez,[39] P. Vazquez Regueiro,[40] C. Vázquez Sierra,[42] S. Vecchi,[21] J. J. Velthuis,[48] M. Veltri,[22,v] A. Venkateswaran,[62] M. Veronesi,[32] M. Vesterinen,[50] D. Vieira,[59] M. Vieites Diaz,[43] X. Vilasis-Cardona,[74] E. Vilella Figueras,[54] A. Villa,[20] P. Vincent,[13] F. C. Volle,[11] D. vom Bruch,[10] A. Vorobyev,[38] V. Vorobyev,[38] N. Voropaev,[38] K. Vos,[73] C. Vrahas,[52] R. Waldi,[17] J. Walsh,[29] G. Wan,[5] C. Wang,[17] J. Wang,[5] J. Wang,[4] J. Wang,[3] J. Wang,[67] M. Wang,[5] R. Wang,[48] X. Wang,[66] Y. Wang,[7] Z. Wang,[44] Z. Wang,[3] Z. Wang,[6] J. A. Ward,[50,63] N. K. Watson,[47] D. Websdale,[55] Y. Wei,[5] C. Weisser,[58] B. D. C. Westhenry,[48] D. J. White,[56] M. Whitehead,[53] A. R. Wiederhold,[50] D. Wiedner,[15] G. Wilkinson,[57] M. K. Wilkinson,[59] I. Williams,[49] M. Williams,[58] M. R. J. Williams,[52] R. Williams,[49] F. F. Wilson,[51] W. Wislicki,[36] M. Witek,[35] L. Witola,[17] C. P. Wong,[61] G. Wormser,[11] S. A. Wotton,[49] H. Wu,[62] K. Wyllie,[42] Z. Xiang,[6] D. Xiao,[7] Y. Xie,[7] A. Xu,[5] J. Xu,[6] L. Xu,[3] L. Xu,[3] M. Xu,[50] Q. Xu,[6] Z. Xu,[9] Z. Xu,[6] D. Yang,[3] S. Yang,[6] Y. Yang,[6] Z. Yang,[5] Z. Yang,[60] L. E. Yeomans,[54] H. Yin,[7] J. Yu,[65] X. Yuan,[62] E. Zaffaroni,[43] M. Zavertyaev,[16] M. Zdybal,[35] O. Zenaiev,[42] M. Zeng,[3] C. Zhang,[5] D. Zhang,[7] L. Zhang,[3] S. Zhang,[65] S. Zhang,[5] Y. Zhang,[5] Y. Zhang,[57] A. Zharkova,[38] A. Zhelezov,[17] Y. Zheng,[6] T. Zhou,[5] X. Zhou,[6] Y. Zhou,[6] V. Zhovkovska,[11] X. Zhu,[3] X. Zhu,[7] Z. Zhu,[6] V. Zhukov,[14,38] Q. Zou,[4,6] S. Zucchelli,[20,f] D. Zuliani,[28] and G. Zunica[56]

(LHCb Collaboration)

[1]*Centro Brasileiro de Pesquisas Físicas (CBPF), Rio de Janeiro, Brazil*
[2]*Universidade Federal do Rio de Janeiro (UFRJ), Rio de Janeiro, Brazil*
[3]*Center for High Energy Physics, Tsinghua University, Beijing, China*
[4]*Institute Of High Energy Physics (IHEP), Beijing, China*
[5]*School of Physics State Key Laboratory of Nuclear Physics and Technology, Peking University, Beijing, China*
[6]*University of Chinese Academy of Sciences, Beijing, China*
[7]*Institute of Particle Physics, Central China Normal University, Wuhan, Hubei, China*
[8]*Université Savoie Mont Blanc, CNRS, IN2P3-LAPP, Annecy, France*
[9]*Université Clermont Auvergne, CNRS/IN2P3, LPC, Clermont-Ferrand, France*
[10]*Aix Marseille University, CNRS/IN2P3, CPPM, Marseille, France*
[11]*Université Paris-Saclay, CNRS/IN2P3, IJCLab, Orsay, France*
[12]*Laboratoire Leprince-Ringuet, CNRS/IN2P3, Ecole Polytechnique, Institut Polytechnique de Paris, Palaiseau, France*
[13]*LPNHE, Sorbonne Université, Paris Diderot Sorbonne Paris Cité, CNRS/IN2P3, Paris, France*
[14]*I. Physikalisches Institut, RWTH Aachen University, Aachen, Germany*
[15]*Fakultät Physik, Technische Universität Dortmund, Dortmund, Germany*
[16]*Max-Planck-Institut für Kernphysik (MPIK), Heidelberg, Germany*
[17]*Physikalisches Institut, Ruprecht-Karls-Universität Heidelberg, Heidelberg, Germany*
[18]*School of Physics, University College Dublin, Dublin, Ireland*
[19]*INFN Sezione di Bari, Bari, Italy*
[20]*INFN Sezione di Bologna, Bologna, Italy*
[21]*INFN Sezione di Ferrara, Ferrara, Italy*
[22]*INFN Sezione di Firenze, Firenze, Italy*
[23]*INFN Laboratori Nazionali di Frascati, Frascati, Italy*
[24]*INFN Sezione di Genova, Genova, Italy*
[25]*INFN Sezione di Milano, Milano, Italy*
[26]*INFN Sezione di Milano-Bicocca, Milano, Italy*
[27]*INFN Sezione di Cagliari, Monserrato, Italy*
[28]*Università degli Studi di Padova, Università e INFN, Padova, Padova, Italy*
[29]*INFN Sezione di Pisa, Pisa, Italy*
[30]*INFN Sezione di Roma La Sapienza, Roma, Italy*

[31]*INFN Sezione di Roma Tor Vergata, Roma, Italy*
[32]*Nikhef National Institute for Subatomic Physics, Amsterdam, Netherlands*
[33]*Nikhef National Institute for Subatomic Physics and VU University Amsterdam, Amsterdam, Netherlands*
[34]*AGH—University of Science and Technology, Faculty of Physics and Applied Computer Science, Kraków, Poland*
[35]*Henryk Niewodniczanski Institute of Nuclear Physics Polish Academy of Sciences, Kraków, Poland*
[36]*National Center for Nuclear Research (NCBJ), Warsaw, Poland*
[37]*Horia Hulubei National Institute of Physics and Nuclear Engineering, Bucharest-Magurele, Romania*
[38]*Affiliated with an institute covered by a cooperation agreement with CERN*
[39]*ICCUB, Universitat de Barcelona, Barcelona, Spain*
[40]*Instituto Galego de Física de Altas Enerxías (IGFAE), Universidade de Santiago de Compostela, Santiago de Compostela, Spain*
[41]*Instituto de Fisica Corpuscular, Centro Mixto Universidad de Valencia—CSIC, Valencia, Spain*
[42]*European Organization for Nuclear Research (CERN), Geneva, Switzerland*
[43]*Institute of Physics, Ecole Polytechnique Fédérale de Lausanne (EPFL), Lausanne, Switzerland*
[44]*Physik-Institut, Universität Zürich, Zürich, Switzerland*
[45]*NSC Kharkiv Institute of Physics and Technology (NSC KIPT), Kharkiv, Ukraine*
[46]*Institute for Nuclear Research of the National Academy of Sciences (KINR), Kyiv, Ukraine*
[47]*University of Birmingham, Birmingham, United Kingdom*
[48]*H.H. Wills Physics Laboratory, University of Bristol, Bristol, United Kingdom*
[49]*Cavendish Laboratory, University of Cambridge, Cambridge, United Kingdom*
[50]*Department of Physics, University of Warwick, Coventry, United Kingdom*
[51]*STFC Rutherford Appleton Laboratory, Didcot, United Kingdom*
[52]*School of Physics and Astronomy, University of Edinburgh, Edinburgh, United Kingdom*
[53]*School of Physics and Astronomy, University of Glasgow, Glasgow, United Kingdom*
[54]*Oliver Lodge Laboratory, University of Liverpool, Liverpool, United Kingdom*
[55]*Imperial College London, London, United Kingdom*
[56]*Department of Physics and Astronomy, University of Manchester, Manchester, United Kingdom*
[57]*Department of Physics, University of Oxford, Oxford, United Kingdom*
[58]*Massachusetts Institute of Technology, Cambridge, Massachusetts, USA*
[59]*University of Cincinnati, Cincinnati, Ohio, USA*
[60]*University of Maryland, College Park, Maryland, USA*
[61]*Los Alamos National Laboratory (LANL), Los Alamos, New Mexico, USA*
[62]*Syracuse University, Syracuse, New York, USA*
[63]*School of Physics and Astronomy, Monash University, Melbourne, Australia (associated with Department of Physics, University of Warwick, Coventry, United Kingdom)*
[64]*Pontifícia Universidade Católica do Rio de Janeiro (PUC-Rio), Rio de Janeiro, Brazil (associated with Universidade Federal do Rio de Janeiro (UFRJ), Rio de Janeiro, Brazil)*
[65]*Physics and Micro Electronic College, Hunan University, Changsha City, China (associated with Institute of Particle Physics, Central China Normal University, Wuhan, Hubei, China)*
[66]*Guangdong Provincial Key Laboratory of Nuclear Science, Guangdong-Hong Kong Joint Laboratory of Quantum Matter, Institute of Quantum Matter, South China Normal University, Guangzhou, China (associated with Center for High Energy Physics, Tsinghua University, Beijing, China)*
[67]*School of Physics and Technology, Wuhan University, Wuhan, China (associated with Center for High Energy Physics, Tsinghua University, Beijing, China)*
[68]*Departamento de Fisica, Universidad Nacional de Colombia, Bogota, Colombia (associated with LPNHE, Sorbonne Université, Paris Diderot Sorbonne Paris Cité, CNRS/IN2P3, Paris, France)*
[69]*Universität Bonn—Helmholtz-Institut für Strahlen und Kernphysik, Bonn, Germany (associated with Physikalisches Institut, Ruprecht-Karls-Universität Heidelberg, Heidelberg, Germany)*
[70]*Eotvos Lorand University, Budapest, Hungary (associated with European Organization for Nuclear Research (CERN), Geneva, Switzerland)*
[71]*INFN Sezione di Perugia, Perugia, Italy (associated with INFN Sezione di Ferrara, Ferrara, Italy)*
[72]*Van Swinderen Institute, University of Groningen, Groningen, Netherlands (associated with Nikhef National Institute for Subatomic Physics, Amsterdam, Netherlands)*
[73]*Universiteit Maastricht, Maastricht, Netherlands (associated with Nikhef National Institute for Subatomic Physics, Amsterdam, Netherlands)*
[74]*DS4DS, La Salle, Universitat Ramon Llull, Barcelona, Spain (associated with ICCUB, Universitat de Barcelona, Barcelona, Spain)*
[75]*Department of Physics and Astronomy, Uppsala University, Uppsala, Sweden (associated with School of Physics and Astronomy, University of Glasgow, Glasgow, United Kingdom)*

[76]*University of Michigan, Ann Arbor, Michigan, USA*
*(associated with Syracuse University, Syracuse, NY, USA)*

[a]Deceased.
[b]Also at Università di Firenze, Firenze, Italy.
[c]Also at Scuola Normale Superiore, Pisa, Italy.
[d]Also at Università di Ferrara, Ferrara, Italy.
[e]Also at Università di Milano Bicocca, Milano, Italy.
[f]Also at Università di Bologna, Bologna, Italy.
[g]Also at Università di Genova, Genova, Italy.
[h]Also at Universidad Nacional Autónoma de Honduras, Tegucigalpa, Honduras.
[i]Also at Università di Bari, Bari, Italy.
[j]Also at Università di Cagliari, Cagliari, Italy.
[k]Also at Università di Roma Tor Vergata, Roma, Italy.
[l]Also at Universidade de Brasília, Brasília, Brazil.
[m]Also at Hangzhou Institute for Advanced Study, UCAS, Hangzhou, China.
[n]Also at Università di Siena, Siena, Italy.
[o]Also at Università degli Studi di Milano, Milano, Italy.
[p]Also at Central South University, Changsha, China.
[q]Also at Università di Padova, Padova, Italy.
[r]Also at Università di Perugia, Perugia, Italy.
[s]Also at Excellence Cluster ORIGINS, Munich, Germany.
[t]Also at Università di Pisa, Pisa, Italy.
[u]Also at Università della Basilicata, Potenza, Italy.
[v]Also at Università di Urbino, Urbino, Italy.